by children aged 9-20 years old are considerably higher than the 1940 RDAs, although the RDAs for protein intake have decreased to approximately 50-70% of the 1940 RDAs.[8] Prior to the war, protein malnutrition was common and thus recommendations for protein intake were high. The 2005 RDAs for protein represent recommended intake for a healthy, well-nourished population. However, the 2005 RDAs for energy intake were estimated average requirements (see Sasaki, this volume) and may be overestimates, given the decreasing activity levels and trends toward overweight and obesity in much of the Japanese population. The additional energy consumed, derived primarily from excess fats and carbohydrates, may be responsible in part for the increased numbers of obese children and may foreshadow an obesity epidemic in Japan.[9] It is important to clearly distinguish between RDAs (population based data for assessment by nutritionists and other scientific professionals) and dietary guidelines (for use by dieticians and the general population to achieve individual health and nutrition).

Similar changes have been observed worldwide over the past 20 years, with a marked shift to diets high in saturated fat, added sugar and refined foods affecting disease trends in many countries, especially in developing countries. Projections for causes of death suggest that while progress is being made in preventing and treating infection, pregnancy-related problems and injuries, lifestyle diseases such as cardiovascular disease and cancer will continue to be the major causes of death in developed countries and also will become major causes of death in developing countries.[10] Currently, a growing number of developing countries face "the double burden of malnutrition": the persistence of undernutrition along with the rapid rise of overnutrition and chronic diseases.

PREVENTION OF DISEASES THROUGH GOOD DIETARY HABITS

The latter half of the 20th century witnessed a paradigm shift concerning nutrition with a focus on overconsumption and an increase in lifestyle-related diseases displacing undernutrition as the primary nutritional concern and challenge facing nutrition scientists and public health workers. At the beginning of the 21st century, dramatic increases in obesity and associated lifestyle related diseases have led to health programs ranging from the global to local levels. The World Health Organization (WHO) launched the WHO Global strategy on Diet, Physical Activity and Health in 2004.[11] In Japan, one of the primary aims of the 10 year national plan for health promotion 'Health Japan 21' promotes maintenance of appropriate body weight (obesity control and prevention of thinness brought about by dieting in young women).[12] However, as the midterm report documents, with an overweight prevalence of 29.0% in males aged 20-60 and 24.6% in females aged 40-60, Japan is far from reaching its targets of an overweight prevalence of less than 15% and 20% in men and women respectively.[13] From 1950 to 1980, energy intake stayed relatively constant but energy derived from fat more than tripled (7.7% to 23.6%) and then leveled off.[14] It is especially noteworthy that while fat from all sources increased, animal-derived fat increased by almost 4-fold.[14] Although the economic burden of lifestyle-related diseases is already high and increasing, financial resources for public health prevention efforts fall far short of those needed to avoid epidemics of metabolic-syndrome related diseases.

In response to these disturbing trends, governments throughout the world have produced various food guidelines (Fig. 2). Ideally these guidelines should reflect countries' cuisines and socio-economic situation, and be tailored to their populations' needs. Indeed, the design and visual image of the Food Guides often reflects a country's culture (e.g. *koma* in Japan, pagoda in Korea and China, pot in Guatemala).[15] However, most of these guidelines have been modifications of the nutritional guidelines developed in the US, which in turn reflect both nutritional science and food industry influence as they were produced primarily by the Department of Agriculture.[16] Now, there is an urgent need to develop a Nutrition Network in Asia so that nutritional scientists can collaborate by exchanging information and data on their commonalities and differences to create nutrition guidelines that reflect the rich food histories of their cultures and meet the varied needs of their populations. Drawing on the healthy traditional food and dietary patterns of Asia, and as an outgrowth of a conference series, "Public Health Implications of Traditional Diets," jointly organized by Harvard School of Public Health, a United Nations World Health Organization/Food and Agriculture Organization (WHO/FAO) Collaborating Center, and Oldways Preservation Trust in 1993, the traditional healthy Asian Diet Pyramid (Fig. 3) provides an example of a nutritional guideline that incorporates both the healthy nutritional history of Asia as well as clinical and epidemiological nutritional-science informed dietary recommendations.[17]

In Japan, the 2000 Dietary Guidelines for Japanese were established jointly by the Ministry of Health, Labour and Welfare (MHLW); the Ministry of Agriculture, Forestry and Fisheries (MAFF); and the Ministry of Education, Culture, Sports, Science and Technology (MEXT). In 2005 in order to disseminate the information more widely to the general population, a Japanese Food Guide "Japanese Food Guide Spinning Top" (Fig. 4) was produced jointly by MHLW and MAFF.[18] It was intended to be used not only as a tool for nutrition education at the community level, but also for food system industries, and representatives were involved from the early stages of its creation. Also in 2005, the Basic Act on *Shokuiku* (in Japanese, *shoku* means 'eating' and *iku* means 'growth/education') promoted the introduction of the "Japanese Food Guide Spinning Top" food and nutrition education for children, as well as for their families.[19]

There is a long history of integrated or holistic approaches to nutrition in Japan. *Shokuiku* is one component of the traditional 4-prong approach to health that also includes an emphasis on knowledge, virtue and physical well-being. The 2005 *Shokuiku* Act and its associated programs integrate eating education in the home/family, school, and local community (government, non-profit organizations, companies, etc). This integration is believed to be essential to achieve significant behavioral changes on an individual and social level. Effective confrontation of the epidemic of obesity and lifestyle

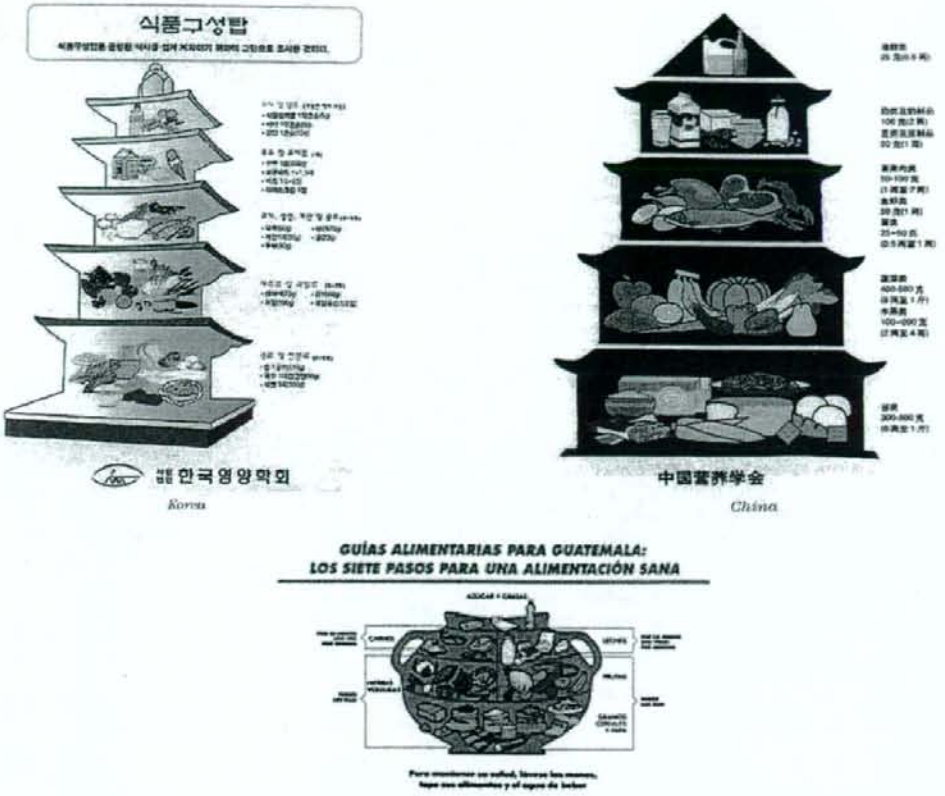

Figure 2. Food pyramids from around the world

Figure 3. Traditional healthy Asian diet pyramid

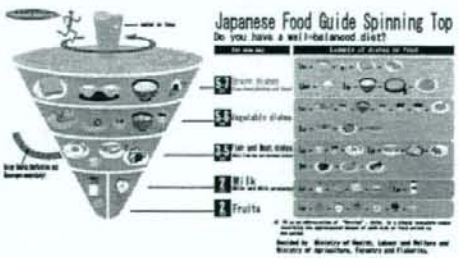

Figure 4. Japanese food guide spinning top

diseases cannot be achieved with narrowly focused programs, but requires an integrated approach such as that embodied in *Shokuiku*.

WHAT IS OUR GOAL?

Japan currently has the longest life expectancy rates in the world (mean of 85.33 years for women in 2003).[20] Yet with increasing rates of lifestyle diseases, life expectancy

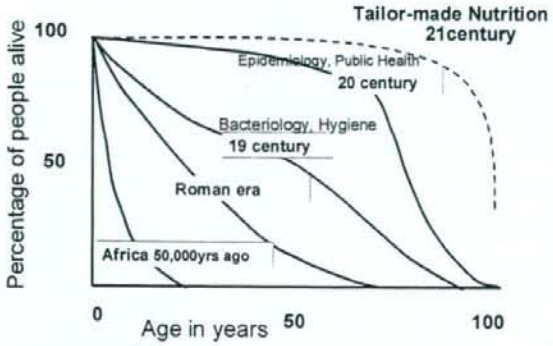

Figure 5. Elongation of life in human history

and quality of life are likely to decrease. Our aim is to extend life expectancy and enhance quality of life through tailor-made nutrition and public health education (Fig. 5). We aim to educate and train nutrition professionals that can provide information and guidance utilizing Dietary Reference Intakes (DRIs) and Nutrition and Food Guidelines but also be tailored to each individual's needs, thereby promoting health among the entire population.

AUTHOR DISCLOSURES

Melissa K Melby, Megumi Utsugi, Miki Miyoshi and Shaw Watanabe, no conflicts of interest.

REFERENCES

1. Saiki T. Nutrition. Tokyo: Eiyosha (Nutrition Co.), 1966.
2. Saiki T. Progress of the Science of Nutrition in Japan. Geneva: League of Nations, 1926.
3. National Institute of Health and Nutrition Japan. History of the National Nutrition Survey in Japan (Japanese) Accessed 21 Jan 2008 at: http://www.nih.go.jp/eiken/chosa/kokumin_eiyou/abou_kokugen.html
4. Association for Improvement of Nutrition. History of major activities (Japanese) Accessed 5 Feb 2008 at: http://www.fukyukai.jp/
5. Japanese Cabinet Office. National Economic Accounting 2003 (in Japanese), 2004.
6. Yoshiike N, Seino F, Tajima S, Arai Y, Kawano M, Furuhata T, Inoue S. Twenty-year changes in the prevalence of overweight in Japanese adults: the National Nutrition Survey 1976-95. Obes Rev. 2002;3(3):183-90.
7. WHO. Public Health Policy and Approaches for Noncommunicable Disease Prevention and Control in Japan: a case study. Japan: WHO Centre for Health Development, 2006.
8. Sasaki S. Dietary Reference Intakes for Japanese (2005): The report from the scientific committee of 'Dietary reference intakes for Japanese - recommended dietary allowance', 2005.
9. Matsushita Y, Yoshiike N, Kaneda F, Yoshita K, Takimoto H. Trends in childhood obesity in Japan over the last 25 years from the national nutrition survey. Obes Res. 2004; 12(2):205-14.
10. WHO. Obesity: Preventing and Managing the Global Epidemic. Geneva: World Health Organization, 2000.
11. WHO. Global Strategy on Diet, Physical Activity and Health. Geneva: World Health Organization, 2004.
12. Yoshiike N, Kaneda F, Takimoto H. Epidemiology of obesity and public health strategies for its control in Japan. Asia Pac J Clin Nutr. 2002;11 Suppl 8:S727-31.
13. Japanese Ministry of Health, Labour and Welfare. Midterm evaluation report of Health Japan 21, 2006.
14. Kida K, Ito T, Yang SW, Tanphaichitr V. Effects of Western diet on risk factors of chronic diseases in Asia. In: Bendich A, Deckelbaum R, eds. Preventive Nutrition: The Comprehensive Guide for Health Professionals. Totowa, NJ: Humana Press, 1997: 523-535.
15. FAO. Food Guidelines by country. Accessed 7 Nov 07 at: http://www.fao.org/ag/agn/nutrition/education_guidelinescountry_en.stm
16. Nestle M. Food Politics: How the food industry influences nutrition and health. Berkeley: University of California Press, 2002.
17. Oldways Preservation & Exchange Trust. The Traditional Healthy Asian Diet Pyramid, 2000. Accessed 16 Oct 07 at: http://www.oldwayspt.org/asian_pyramid.html
18. Japanese Ministry of Health, Labour and Welfare. About "Japanese Food Guide Spinning Top" Accessed 7 Nov 07 at: http://www.mhlw.go.jp/bunya/kenkou/eiyou-syokuji. html
19. Yoshiike N, Hayashi F, Takemi Y, Mizoguchi K, Seino F. A new food guide in Japan: the Japanese food guide Spinning Top. Nutr Rev. 2007;65(4):149-54.
20. Japanese Ministry of Health, Labour and Welfare. Summary of Vital Statistics: Japanese Ministry of Health, Labour and Welfare, 2003. Accessed 12 March 2005 at: http://www.mhlw.go.jp/english/database/db-hw/populate/ pop4.html

Arteriosclerosis, Thrombosis, and Vascular Biology

JOURNAL OF THE AMERICAN HEART ASSOCIATION

American Heart Association®

Learn and Live℠

Cilostazol Inhibits Oxidative Stress Induced Premature Senescence Via Upregulation of Sirt1 in Human Endothelial Cells

Hidetaka Ota, Masato Eto, Mitsunobu R. Kano, Sumito Ogawa, Katsuya Iijima, Masahiro Akishita and Yasuyoshi Ouchi

Arterioscler. Thromb. Vasc. Biol. 2008;28;1634-1639; originally published online Jun 12, 2008;
DOI: 10.1161/ATVBAHA.108.164368
Arteriosclerosis, Thrombosis, and Vascular Biology is published by the American Heart Association. 7272 Greenville Avenue, Dallas, TX 72514
 Print ISSN: 1079-5642. Online ISSN: 1524-4636

Cilostazol Inhibits Oxidative Stress–Induced Premature Senescence Via Upregulation of Sirt1 in Human Endothelial Cells

Hidetaka Ota, Masato Eto, Mitsunobu R. Kano, Sumito Ogawa, Katsuya Iijima, Masahiro Akishita, Yasuyoshi Ouchi

Objective—Cilostazol, a selective inhibitor of PDE3, has a protective effect on endothelium after ischemic vascular damage, through production of nitric oxide (NO). The purpose of the present study was to clarify the molecular mechanisms underlying the preventive effect of treatment with cilostazol on oxidative stress–induced premature senescence in human endothelial cells.

Methods and Results—Prematurely senescent human umbilical vein endothelial cells (HUVECs) were induced by treatment with hydrogen peroxide (H_2O_2) as judged by senescence-associated β-galactosidase assay (SA-βgal), cell morphological appearance, and plasminogen activator inhibitor-1 (PAI-1) expression. Treatment with H_2O_2 caused 93% of the cells to be SA-βgal positive, whereas 46% of cilostazol (100 μmol/L)-treated cells were positive. HUVECs treated with other cAMP-elevating agents and DETA-NO showed a reduction of SA-βgal–positive cells as well. Cilostazol increased phosphorylation of Akt at Ser^{473} and of endothelial nitric oxide synthase (eNOS) at Ser^{1177}, with a dose-dependent increase in Sirt1 expression. Moreover, the effect of cilostazol on premature senescence was abrogated through inhibition of Sirt1.

Conclusions—Our results indicated that cilostazol exerted protective effects against endothelial senescence and dysfunction, and enhancement of NO production is a key mediator in upregulation of Sirt1. (***Arterioscler Thromb Vasc Biol.* 2008;28:1634-1639**)

Key Words: cilostazol ■ eNOS ■ Sirt1 ■ endothelial senescence

The phenomenon of human aging is known to be a critical cardiovascular risk factor. Cellular senescence of endothelial cells has been proposed to be involved in endothelial dysfunction and atherogenesis.[1] The lesions of human atherosclerosis have been extensively studied histologically, and these studies have demonstrated that there are vascular cells that exhibit the morphological features of cellular senescence.[2]

See accompanying article on page 1577

The telomere hypothesis is a widely accepted explanation of the occurrence of cellular senescence.[3] Cessation of cell division after extended propagation in culture for a few weeks or months is related to the attrition of telomeres, which is termed replicative senescence. In addition to telomere attrition, some stressors such as oxidative stress elicit similar growth arrest within just a few days, referred to as stress-induced premature senescence (SIPS). Both types of senescence are accompanied by a specific set of changes in cell function, morphology, and gene expression.[4] In addition to the above changes, recognized biomarkers of senescent cells include staining for β-galactosidase at pH of 6.0 as opposed to endogenous lysosomal enzyme detected at pH of 4.0 in normal cells.[5]

According to the free-radical theory, reactive oxygen species (ROS) may be potential candidates responsible for senescence and age-related diseases, and on production of high levels of ROS, the redox balance is disturbed and cells shift into a state of oxidative stress, which subsequently leads to premature senescence with shortening telomeres.[6]

A PDE3 inhibitor, cilostazol, is used as a vasodilating antiplatelet drug for treating intermittent claudication, and in preclinical studies was shown to have a protective effect on endothelial cells by increasing eNOS activity.[7] Cilostazol increases intracellular cAMP content accordingly and activates protein kinase A (PKA) or PI3K/Akt signaling.[8] As recently shown, endothelial NO can protect against a state of oxidative stress, and activation of eNOS and subsequent production of NO delay endothelial cellular senescence.[9,10]

In yeast, Sir2 (silent information regulator-2) has been identified as an NAD^+-dependent histone deacetylase.[11]

Original received February 4, 2008; final version accepted May 28, 2008.

From the Departments of Geriatric Medicine (H.O., M.E., S.O., K.I., M.A., Y.O.) and Molecular Pathology (M.R.K.), Graduate School of Medicine, University of Tokyo, Japan.

Correspondence to Yasuyoshi Ouchi, MD, PhD, Department of Geriatric Medicine, Graduate School of Medicine, The University of Tokyo, 7-3-1 Hongo, Bunkyo-ku, Tokyo 113-8655, Japan. E-mail youchi-tky@umin.ac.jp

Arterioscler Thromb Vasc Biol **is available at http://atvb.ahajournals.org** **DOI: 10.1161/ATVBAHA.108.164368**

Mammalian sirtuin 1 (Sirt1), the closest homolog of Sir2, regulates the cell cycle, senescence, apoptosis, and metabolism, by interacting with a number of molecules, including p53, PML, and PPAR-γ.[12–14] A recent study showed that production of NO by caloric restriction increases Sirt1 expression and suggested that eNOS may be involved in regulating the expression of Sirt1 in murine white adipocytes.[15] Therefore, we consider that the protective effect of cilostazol against vascular senescence may be attributed to upregulation of Sirt1.

In the present study, cilostazol inhibited oxidative stress–induced premature senescence, and the increased expression of Sirt1 by this drug played a critical role in prevention of endothelial senescence.

Materials and Methods

Cilostazol was kindly provided by Otsuka Pharmaceutical Co Ltd, Tokyo, Japan. Forskolin, rolipram, N^G-nitro-L-arginine methyl ester hydrochloride (L-NAME) and LY294002 were purchased from Sigma. Myristoylated cell-permeable PKA inhibitor peptide sequence[14–22] amide (PKAI) was from Alexis Biochemicals. (Z)-1-[2-(2-aminoethyl)-N-(2-ammonioethyl)amino] diazen-1-IM1,2 diolate (DETA-NO), S-nitrosoacetyl penicillamine (SNAP), 8 Br-cGMP, and 8 Br-cAMP were from Cayman Chemical. *N*-acetyl-cystein (NAC) was purchased from Calbiochemo.

Cell Culture

Human umbilical vein endothelial cells (HUVECs) were purchased from CAMBREX (Walkersville, Md), and maintained in endothelial growth medium (EGM-2, EGM-2 singleQuots, CAMBREX). Population doubling levels (PDL) were calculated as described previously,[16] and all experiments were performed at PDL of 8 to 9.

Measurement of cAMP Level

HUVECs were plated in 96-well plates at a density of 5×10^3 cells per well and cultured overnight. After 15-minute incubation with cilostazol, the medium was aspirated and a lysis buffer was added. cAMP concentration was determined using a cAMP EIA kit (Amersham Biosciences) according to the manufacturer's instructions.

Inhibition of Sirt1

Proliferating cells were washed 3 times with growth medium and exposed for 24 hours to the indicated concentrations of sirtinol (Calbiochem) or nicotinamide (NAM, Wako Chemical Industries) diluted in medium. After exposure, the dishes were washed 3 times with inhibitor-free medium and cultured. Proliferating cells were transfected with 200 pmol/L siRNA for Sirt1 (GAT GAA GTT GAC CTC CTC A[14] and TGA AGT GCC trichloroacetic acid (TCA) GAT ATT A) or control siRNA (Darmacom Co.) using silMPORTER (Upstate Cell Signaling Solutions).

Senescence-Associated β-Galactosidase (SA-βgal) Staining

HUVECs were grown in 100-mm collagen-coated dishes to 80% confluence. HUVECs were pretreated with vehicle (0.05% DMSO), cilostazol (1 to 100 μmol/L), forskolin (0.1 to 1 μmol/L), rolipram (10 to 100 μmol/L), DETA-NO (50, 100 μmol/L), or NAC (3, 5 mmol/L) diluted in EGM-2 medium for 3 days. HUVECs were washed 3 times with EGM-2 and then treated for 1 hour with 100 μmol/L H_2O_2 diluted in EGM-2. After the treatment, HUVECs were trypsinized, reseeding at the density of 1×10^5 in 60-mm dishes and cultured with EGM-2 containing these compounds for 10 days. At 10 days after treatment with H_2O_2, HUVECs were fixed and the proportion of SA-βgal–positive cells was determined as described by Dimri et al.[5]

NOS Activation Assay

NOS activity was determined using an NOS assay kit (Calbiochem) according to the manufacturer's instructions.

BrdU Incorporation Assay

BrdU incorporation was analyzed using a commercial kit (Roche).

Immunoblotting

Cells were lysed on ice for 1 hour in buffer (50 mmol/L Tris-HCl, pH 7.6, 150 mmol/L NaCl, 1%NP-40, 0.1%SDS, 1 mmol/L dithiothreitol, 1 mmol/L sodium vanadate, 1 mmol/L phenylmethylsulfonyl fluoride, 10 μg/mL aprotinin, 10 μg/mL leupeptin, and 10 mmol/L sodium fluoride). Equal amounts of protein were separated by SDS-polyacrylamide gel electrophoresis and transferred to nitrocellulose membranes. After blocking, the filters were incubated with the following antibodies; antiphospho-eNOS (Ser1177), antiphospho-Akt (Ser473), anti-Akt (Cell Signaling Technology), antieNOS (BD Transduction Laboratories), antiacetyl-p53 (Lys373/382), antip53, anti-Sirt1 (Santa Cruz Biotechnology Inc), anti-PAI-1 (Molecular Innovations Inc), and anti-β-actin (Sigma). After washing and incubation with horseradish peroxidase-conjugated antirabbit or antimouse IgG (Amersham) for 1 hour, the antigen-antibody complexes were visualized using an enhanced chemiluminescence system (Amersham).

Real-Time Quantitative Reverse Transcription

Expression of Sirt1 in HUVECs was measured by quantitative RT-polymerase chain reaction (PCR). Total RNA in HUVECs was isolated with ISOGEN (Nippon gene Inc). After treatment with Rnase-free Dnase for 30 minutes, total RNA (50 ng/μL) was reverse transcribed with random hexamers and oligo d(T) primers. The expression level of Sirt1 relative to GAPDH was determined by means of staining with SYBR green dye and a LineGene fluorescent quantitative detection system (Bioflux Co), as recommended by the manufacturer. Primer quality was verified by dissociation curve analysis, the slopes of standard curves, and reactions without RT. The following primers were used: Sirt1 (forward (F) 5′-CCTGACTTCAGATCAAGAGACGGT-3′; reverse (R) 5′-CTGATTAAAAATGTCTCCACGAACAG-3′, GAPDH F 5′-ACCAC-AGTCCATGCCATCAC-3′; R 5′-TCCACCACCCTGTTGCTGTA-3′).

Animal Experiments

The animal experiments were approved by our institutional review board. Ten-week-old SPF male wild-type BALB/c mice (n=40, weighing approximately 25 g) were supplied by Charles River Laboratories Inc. Animals were housed under a 12-hour light/dark cycle and fed a normal diet. These mice were administered 25 mg/kg paraquat (1,1-dimethyl-4,4-bipyridinium) (Wako Chemical) by intraperitoneal injection. Then mice were randomly assigned to 2 treatment groups (control group, n=20; cilostazol group, n=20). The each group received gavage administration of vehicle alone or cilostazol 60 mg/kg/d for their lifetime. We made diabetic mice (n=40) by a single intraperitoneal injection of streptozotocin (STZ; 60 mg/kg, Sigma). Tail blood glucose was assayed 3 days after injection using glucose test strips (Roche). The mice were killed by cervical dislocation. The aorta was removed after systemic perfusion with phosphate-buffered saline (PBS) for histological examination. The proportion of SA-βgal–positive cells was analyzed by NIH image software. The primary antibody was purified rat antimouse CD31 (platelet endothelial cell adhesion molecule; PECAM-1) monoclonal antibody from pharmingen. ROS were measured with 2′, 7′-Dichlorodihydrofluorescein, diacetate (DCF) (Sigma). As previously described by Shi et al,[17] the aorta was rapidly removed and placed in oxygenated (12% O_2, 5% CO_2) physiological salt solution (PSS) of the following composition (NaCl 130 mmol/L, KCl 4.7 mmol/L, $CaCl_2$ 1.6 mmol/L, $MgSO_4$ 1.17 mmol/L, $NaHCO_3$ 14.9 mmol/L, KH_2PO_4 1.18 mmol/L, EDTA 0.026 mmol/L, glucose 1.0 mmol/L). The living aorta was carefully isolated, cannulated (24G, Terumo Co Ltd) at both ends, pressured, and loaded with DCF solution (10 μmol/L) for 10 minutes. Then the aorta was washed by PSS 3 times, embedded in OCT medium, and cryosectioned.

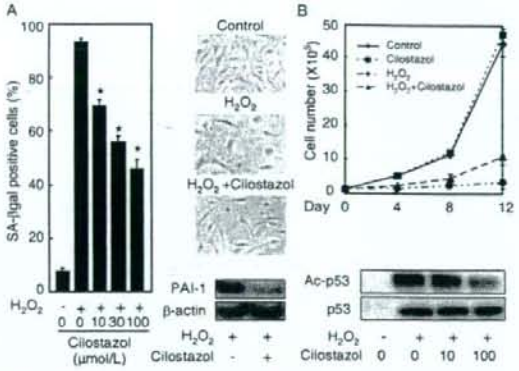

Figure 1. A, Cilostazol inhibited H_2O_2 (100 μmol/L)-induced premature senescent phenotype in HUVECs as judged by SA-βgal staining (*$P<0.05$, n=3), morphological changes, and PAI-1. B, Cell growth curve, acetylation of p53 (Ac-p53) at lysine 373/382, and total protein of p53 were evaluated at 10 days after addition of H_2O_2.

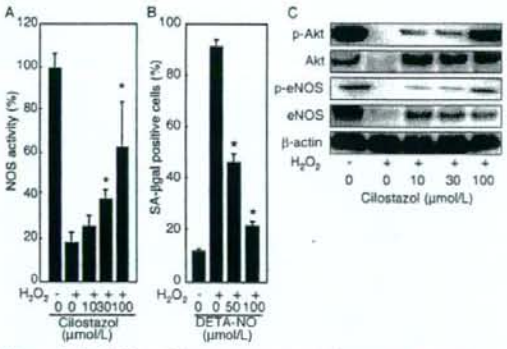

Figure 2. A, NOS activity was measured after treatment with cilostazol. B, DETA-NO inhibited H_2O_2 (100 μmol/L)-induced premature senescent phenotype in HUVECs as judged by SA-βgal staining. (*$P<0.05$, n=3). C, Expression of phospho-eNOS (Ser1177), phospho-Akt (Ser473), Akt, and eNOS in cilostazol-treated cells.

TOTO-3 for nuclear staining, secondary antibodies (Alexa Fluor 488 donkey antirat IgG and Alexa Fluor 594 donkey antirat IgG), and antifade reagent were from Molecular Probe (Invitrogen). Fluorescent images were taken and analyzed using a confocal laser microscope (LSM510, Carl Zeiss MicroImaging Co Ltd). Urinary 8-Hydroxydeoxyguanosine (8-OhdG) and creatinine were measured using a DNA damage ELISA kit (Stressgen) and creatinine assay kit (Cayman chemical), respectively.

Telomerase Assay

Telomerase activity was measured with 2 μg protein using a telomerase PCR-ELISA kit according to the manufactures instructions (Chemicon, Temecula).

Data Analysis

Values are shown as mean±SEM in the text and figures. Differences between the groups were analyzed using 1-way analysis of variance, followed by Bonferroni test. Probability values less than 0.05 were considered significant.

Results

Cilostazol Inhibits Oxidative Stress–Induced Premature Senescence in Human Endothelial Cells

To investigate the effect of cilostazol on the senescent phenotype in HUVECs, we induced premature endothelial senescence by addition of H_2O_2 100 μmol/L for 1 hour. We found that treatment with cilostazol inhibited the senescent phenotype as judged by SA-βgal assay and enlarged and flattened cell morphological appearance at 10 days. Under treatment with H_2O_2, 93% of cells were SA-βgal positive, versus only 46% of cilostazol (100 μmol/L)-treated cells under the same oxidative conditions (Figure 1A). We found that HUVECs treated with other cAMP-elevating agents showed a reduction of SA-βgal–positive cells as well (forskolin 1 μmol/L; 51%, rolipram 100 μmol/L; 53%). Treatment with cilostazol decreased the specific senescent morphological changes (Figure 1A). Expression of PAI-1 was decreased by treatment with cilostazol (Figure 1A). Treatment with cilostazol restored the rate of BrdU incorporation in prematurely senescent HUVECs (supplemental Figure I, available online at http://atvb.ahajournals.org). In parallel with this, telomerase activity was increased by treatment with cilostazol (supplemental Figure I). Moreover, we examined the effect on cell growth for 12 days after treatment with vehicle, H_2O_2 and cilostazol. Addition of H_2O_2 decreased cell number of HUVECs and treatment with cilostazol recovered it (Figure 1B). p53 plays a pivotal role in cellular senescence. Therefore, we examined the expression and acetylation of p53 at Lys373/382, one of the critical targets of Sirt1. As shown in Figure 1B, we observed that H_2O_2 increased the expression and acetylation of p53, and treatment with cilostazol decreased the acetylation of p53.

Enhancement of cAMP Production and eNOS Activity Induced by Cilostazol

When HUVECs were treated with cilostazol, the cAMP level significantly increased in a concentration-dependent manner at cilostazol concentrations of 1 and 100 μmol/L (data not shown). In the presence of H_2O_2, cilostazol increased eNOS activity (Figure 2A), expression of eNOS, and the phosphorylation of eNOS at Ser^{1177} in parallel with the phosphrylation of Akt at Ser^{473} (Figure 2C). Although exposure to H_2O_2 affected the total amount of eNOS and Akt, treatment with cilostazol reverted their expression to nearly normal levels (Figure 2C). To investigate the effect of NO on the senescent phenotype in HUVECs, we treated these cells with an NO donor, DETA-NO (100 μmol/L). DETA-NO–treated HUVECs showed decreased SA-βgal–positive cells (Figure 2B), and an increased rate of BrdU incorporation and telomerase activity (supplemental Figure I). These results suggest that the protective effect against a senescent phenotype may be attributed to an increased of NO via eNOS activation by cilostazol.

Treatment With Cilostazol Increased Sirt1 Expression

To explore the mechanism by which cilostazol prevents from premature endothelial senescence, we considered that an increase in NO production could promote the longevity gene,

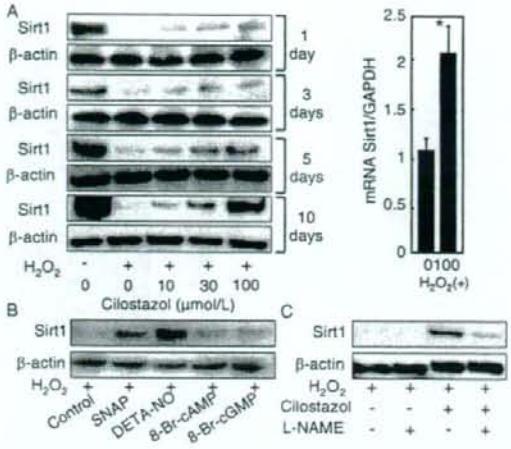

Figure 3. A, Sirt1 protein and mRNA in the presence of H_2O_2 (100 μmol/L). Sirt1 expression was increased by treatment with SNAP (100 μmol/L), DETA-NO (50 μmol/L), 8 Br-cGMP (1 mmol/L), or 8 Br-cAMP (1 mmol/L) (B) and decreased by treatment with L-NAME (20 μmol/L) for 6 hours (C). *$P<0.05$.

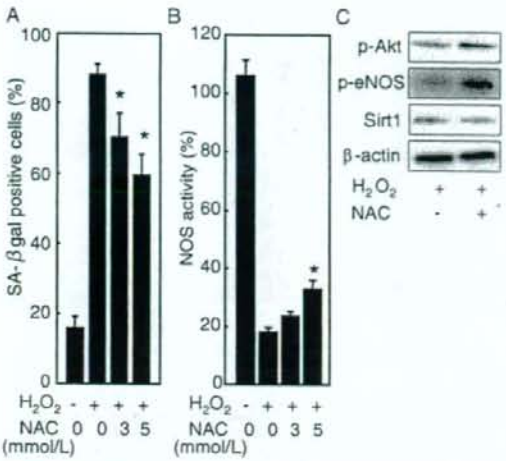

Figure 4. A, Treatment with NAC (0, 3, 5 mmol/L) inhibited H_2O_2 (100 μmol/L)-induced premature senescent phenotype in HUVECs as judged by SA-βgal staining (n=3). B, NOS activity after treatment with NAC. C, Expression of phospho-eNOS (Ser1177), phospho-Akt (Ser473), and Sirt1 in NAC (5 mmol/L)-treated cells. *$P<0.05$.

Sirt1. We found that cilostazol significantly increased Sirt1 mRNA and protein in a concentration-dependent manner for 10 days after treatment with H_2O_2 (Figure 3A). In contrast, Sirt1 mRNA and protein were not altered in the absence of H_2O_2 treatment (data not shown). To determine whether the expression of Sirt1 was regulated by the increase in NO production, we exposed prematurely senescent HUVECs to either an NO donor (such as DETA-NO or SNAP), a cAMP analog (8 Br-cAMP), or a cGMP analog (8 Br-cGMP). After these treatments, the expression of Sirt1 protein was markedly higher than that in untreated cells (Figure 3B). Furthermore, treatment with an NOS inhibitor, L-NAME, decreased Sirt1 expression (Figure 3C). To clarify the molecular mechanisms by which cilostazol induces SIRT1 expression, we examined the effect of protein kinase inhibitors on the cilostazol-induced phosphrylation of eNOS, Akt and expression of Sirt1 (supplemental Figure II). In the absence of H_2O_2 treatment, PKAI and LY294002 inhibited the cilostazol-induced phosphorylation of eNOS at Ser^{1177}. The cilostazol-induced phosphorylation of Akt at Ser^{473} was inhibited by LY294002, however the inhibition by PKAI was not significant. Sirt1 expression was not altered by treatment with PKAI or LY294002. In the presence of H_2O_2 treatment, PKAI and LY294002 showed the similar effect on the cilostazol-induced phosphorylation of eNOS at Ser^{1177} and Akt at Ser^{473}, but Sirt1 expression was significantly decreased.

Cilostazol Dose Not Have a Function of Direct Scavenger of Hydrogen Peroxide

It is possible that cilostazol may function as an antioxidant drug. Therefore, we examined the effect of NAC, another antioxidant, on Sirt1 expression, phosphorylation of Akt, and NOS activity as well as senescence markers. As shown in Figure 4A, treatment with NAC (0, 3, 5mmol/L) significantly decreased SA-βgal activity. Phosphorylation of Akt and NOS activity was increased by treatment with NAC (Figure 4B and 4C). However, Sirt1 expression was not altered (Figure 4C). To clarify the effect of cilostazol or NAC on H_2O_2, we examined whether cilostazol or NAC could scavenge H_2O_2 radicals. We performed a cell-free, horseradish peroxidase–coupled oxidation analysis.[18] We observed that NAC scavenged H_2O_2 significantly, but cilostazol not (supplemental Figure III). These results indicate that inhibiting H_2O_2-induced senescence by cilostazol may not be attributable to its direct antioxidative effect such as NAC.

Inhibition of Sirt1 Abrogates the Protective Effect of Cilostazol Against Premature Senescence

To determine the role of endogenous Sirt1 in premature senescence, HUVECs were treated with a Sirt1 chemical inhibitor, sirtinol, a physiological Sirt1 inhibitor, NAM or Sirt1 siRNA. Knockdown of Sirt1 with siRNA was confirmed by Western blotting. As shown in Figure 5A and 5B, Sirt1 inhibition abrogates the effect of cilostazol on SA-βgal activity and the senescent specific morphological changes. Likewise, we found that Sirt1 inhibition had a similar effect to DETA-NO treatment (data not shown). Increased phosphorylation of eNOS at Ser^{1177} and decreased expression of PAI-1 by cilostazol were no longer observed when Sirt1 was inhibited (Figure 5C). These results indicate that Sirt1 could play an important role in the protective effect of cilostazol against a senescent phenotype.

Administration of Cilostazol Inhibits Vascular Endothelial Senescence Induced by Oxidative Stress in BALB/c Mice

To investigate whether cilostazol has a protective effect on vascular endothelial senescence induced by oxidative stress in vivo, we administrated paraquat, a herbicide that generates

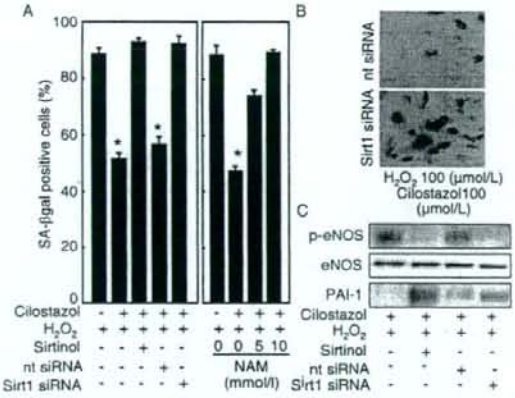

Figure 5. Inhibition of Sirt1 abrogates effect of cilostazol (100 μmol/L) against a premature senescence phenotype as shown by SA-βgal staining (n=3) (A), morphological changes (B), and expression of phospho-eNOS (Ser1177) and PAI-1 (C). Sirt1 was inhibited by sirtinol (100 μmol/L), NAM (5, 10 mmol/L), or Sirt1 siRNA. nt indicates nontargeted. *$P<0.05$.

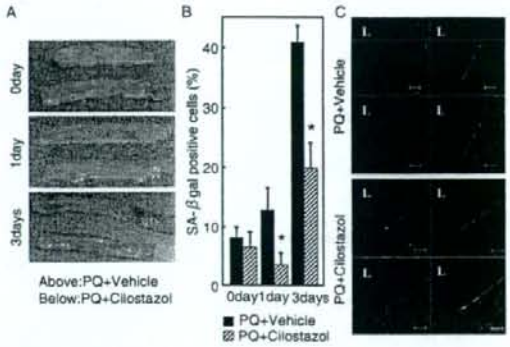

Figure 6. A, SA-βgal staining of thoracic arteries from BALB/c mice with cilostazol at 0, 1, and 3 days after treatment with paraquat (PQ). B, The number of SA-βgal staining cells in cilostazol-treated thoracic arteries. C, Immunofluorescent staining for Sirt1 (green), PECAM-1 (red), and TOTO-3 (blue). Representative samples (n=40) shown. *$P<0.05$.

superoxide, to BALB/c mice. We performed resection of the thoracic artery of these mice and compared the senescent phenotype in the presence and absence of cilostazol. The number of SA-βgal–staining cells was significantly increased in untreated thoracic arteries, but was decreased in cilostazol-treated thoracic arteries (Figure 6A and 6B). Cross-sections of arteries stained with SA-βgal showed that positive cells were mostly located on the luminal surface and stained for CD-31, indicating that blue staining originated from vascular endothelial cells and not from the extracellular matrix (supplemental Figure IV). To estimate the degree of DNA damage caused by paraquat, we measured urinary 8-OhdG, a marker of DNA damage from oxidative stress. Urinary 8-OHdG level was decreased after cilostazol treatment (supplemental Figure IV). Immunostaining of the sections for Sirt1 showed that Sirt1 expression was increased in aortic endothelial cells by treatment with cilostazol (Figure 6C). To estimate the antioxidative effect of cilostazol on vasculature, we used DCF, cell-permeable fluorogenic probe, to measure ROS within cells by detection of enzymatically formed H_2O_2. The intensity of green fluorescence indicating DCF-positive cells was markedly increased in untreated thoracic arteries, which was decreased in cilostazol-treated thoracic arteries (supplemental Figure IV). The number of DCF-positive endothelial cells was decreased in cilostazol-treated thoracic arteries (supplemental Figure IV). Next, we used STZ diabetic mice in which the endothelial senescence documented.[19] The treatment with cilostazol decreased SA-βgal–positive endothelial cells (supplemental Figure V).

Discussion

As previously reported,[20] the concentration of cilostazol (60 mg/kg/d) we administrated in this study was within clinical relevance. In vitro experiments, we used cilostazol at 0 to 100 μmol/L and confirmed a concentration-dependent trend. Given the average plasma concentration of cilostazol orally administered to humans (100 mg/body/d) is about 2 to 10 μmol/L and may be partially higher in our body, our used concentration of cilostazol is comparable to clinical.

Previous studies have shown that overexpression of Sirt1 antagonizes cellular senescence through acetylation of p53 with localization of the PML body.[13] Recently, we reported that Sirt1 overexpression prevented the development of oxidative stress–induced premature senescence in human endothelial cells.[21] Senescence of endothelial cells leads to endothelial dysfunction and may result in advanced atherosclerotic lesions.[2] In fact, it has been reported that endothelial cells in samples of human aortia with atherosclerosis exhibited a senescence-like phenotype, increased expression of PAI-1,[22] and decreased production of NO.[1] NO production and eNOS expression are severely limited in senescent endothelial cells.[23] Although NO is known to be involved in reducing oxidative stress and the progression of atherosclerosis, the present study suggested that the NO-mediated prevention of premature senescence was attributable to Sirt1 function. These findings implicate the NO-Sirt1 axis as one of the fundamental determinants of endothelial senescence, and the role of Sirt1 as a driver of cellular stress resistance and longevity is noteworthy in the context of its expression profile.

The free-radical theory of aging proposes that degenerative senescence is largely the result of the cumulative effect of ROS. In this study, we used paraquat mice as an oxidative stress model. Moreover, we studied the effect of cilostazol on endothelial senescence used by STZ-diabetic mice as more suitable for clinical settings. In addition, Takase et al recently reported that cilostazol had exhibited an antiatherosclerotic effect on vasculature in ApoE-deficient mice.[24] Therefore, we suggest that cilostazol has a beneficial effect on vasculature in clinical settings.

Cilostazol-induced NO production by eNOS activation via a cAMP/PKA- and PI3K/Akt-dependent mechanism was previously confirmed in the porcine thoracic aorta by an ESR[25] technique and in clinical practice by endothelial-dependent vasodilation.[26] Our results showed that cilostazol phosphorylated Akt via a PKA-independent mechanism (sup-

plemental Figure II). It is suggested that both cAMP/PKA and PI3K/Akt signaling pathways are involved in cilostazol-induced phosphorylation of eNOS, however the contribution of these signaling to the upregulation of Sirt1 in the presence of H_2O_2 is more critical than that of in the absence of H_2O_2. Therefore, we suggest that upregulation of Sirt1 by cilostazol is modulated via cAMP/PKA, PI3K/Akt, and eNOS-dependent mechanism under oxidative conditions, but further investigation is needed to elucidate why there is discrepancy of Sirt1 expression.

A recent study showed DETA-NO, an NO-donor, and eNOS transfection activated hTERT and delayed endothelial senescence, indicating that eNOS has an antiatherosclerotic effect even in cases of advanced atherosclerosis. It is therefore suggested that incrased NO bioavailability by other pharmaceutical products such as 3-hydroxy-3-methylglutaryl (HMG)-coenzyme A (CoA) reductase inhibitors or agents with phytoestrogenic properties such as resveratrol may exert a protective effect against endothelial senescence, and this possibility deserves further investigation.

In summary, we showed that cilostazol inhibited oxidative stress–induced premature senescence, and subsequently enhancement of Sirt1 expression played a critical role in inhibition of a senescent phenotype in human endothelial cells. Our results suggest that NO production by cilostazol has a protective effect against endothelial senescence and dysfunction.

Sources of Funding

This work was supported by a Grant-in-Aid for Scientific Research from the Ministry of Education, Science, Culture and Sports of Japan (18590801).

Disclosures

None.

References

1. Minamino T, Miyauci H, Yoshida T, Ishida Y, Yoshida H, Komuro I. Endothelial cell senescence in human atherosclerosis: role of telomere in endothelial dysfunction. *Circulation*. 2002;105:1541–1544.
2. Burrig KF. The endothelium of advanced arteriosclerotic plaques in humans. *Arterioscler Thromb*. 1991;11:1678–1689.
3. Liu JP. Studies of the molecular mechanisms in the regulation of telomerase activity. *FASEB J*. 1999;13:2091–2104.
4. Yang J, Chang E, Cherry AM, Bangs CD, Oei Y, Bodnar A, Bronstein A, Chiu CP, Herron GS. Human endothelial cell life extension by telomerase expression. *J Biol Chem*. 1999;274:26141–26148.
5. Dimri GP, Lee X, Basile G, Acosta M, Scott G, Roskelley C, Medrano EE, Linskens M, Rubelj I, Pereira-Smith O, et al. A biomarker that identifies senescent human cells in culture and in aging skin in vivo. *Proc Natl Acad Sci USA*. 1995;92:9363–9367.
6. Kurz DJ, Decary S, Hong Y, Trivier E, Akhmedov A, Erusalimsky JD. Chronic oxidative stress compromises telomere integrity and accelerates the onset of senescence in human endothelial cells. *J Cell Sci*. 2004;117:2417–2426.
7. Kambayashi J, Liu Y, Sun B, Shakur Y, Yoshitake M, Czerwiec F. Cilostazol as a unique antithrombotic agent. *Curr Pharm Des*. 2003;9:2289–2302.
8. Hashimoto A, Miyakoda G, Hirose Y, Mori T. Activation of endothelial nitric oxide synthase by cilostazol via a cAMP/protein kinase A- and phosphatidylinositol 3-kinase/Akt-dependent mechanism. *Atherosclerosis*. 2006;189:350–357.
9. Hayashi T, Matsui-Hirai H, Miyazaki-Akita A, Fukatsu A, Funami J, Ding QF, Kamalanathan S, Hattori Y, Ignarro LJ, Iguchi A. Endothelial cellular senescence is inhibited by nitric oxide: implications in atherosclerosis associated with menopause and diabetes. *Proc Natl Acad Sci USA*. 2006;103:17018–17023.
10. Vasa M, Breitschopf K, Zeiher AM, Dimmeler S. Nitric oxide activates telomerase and delays endothelial cell senescence. *Circ Res*. 2000;87:540–542.
11. Braunstein M, Rose AB, Holmes SG, Allis CD, Broach JR. Transcriptional silencing in yeast is associated with reduced nucleosome acetylation. *Genes Dev*. 1993;7:592–604.
12. Vaziri H, Dessain SK, Ng Eaton E, Imai SI, Frye RA, Pandita TK, Guarente L, Weinberg RA. hSIR2 (SIRT1) functions as an NAD-dependent p53 deacetylase. *Cell*. 2001;107:149–159.
13. Langley E, Pearson M, Faretta M, Bauer UM, Frye RA, Minucci S, Pelicci PG, Kouzarides T. Human SIR2 deacetylates p53 and antagonizes PML/p53-induced cellular senescence. *EMBO J*. 2002;21:2383–2396.
14. Picard F, Kurtev M, Chung N, Topark-Ngarm A, Senawong T, Machado De Oliveira R, Leid M, McBurney MW, Guarente L. Sirt1 promotes fat mobilization in white adipocytes by repressing PPAR-gamma. *Nature*. 2004;429:771–776.
15. Nisoli E, Tonello C, Cardile A, Cozzi V, Bracale R, Tedesco L, Falcone S, Valerio A, Cantoni O, Clementi E, Moncada S, Carruba MO. Calorie restriction promotes mitochondrial biogenesis by inducing the expression of eNOS. *Science*. 2005;310:314–317.
16. Maciag T, Hoover GA, Stemerman MB, Weinstein R. Serial propagation of human endothelial cells in vitro. *J Cell Biol*. 1981;91:420–426.
17. Shi Y, Man RY, Vanhoutte PM. Two isoforms of cyclooxygenase contribute to augmented endothelium-dependent contractions in femoral arteries of 1-year-old rats. *Acta Pharmacol Sin*. 2008;29:185–192.
18. Frew JE, Jones P, Scoles G. Spectrophotometric determination of hydrogen peroxide and organic hydroperoxides at low concentrations in aqueous solution. *Analytica chemica acta*. 1983;155:139–150.
19. Yokoi T, Fukuo K, Yasuda O, Hotta M, Miyazaki J, Takemura Y, Kawamoto H, IchijoH, Ogihara T. Apoptosis signal-regulating kinase 1 mediates cellular senescence induced by high glucose in endothelial cells. *Diabetes*. 2006;55:1660–1665.
20. Akiyama H, Kudo S, Shimizu T. The absorption, distribution and excretion of a new antithrombotic and vasodilating agent, cilostazol, in rat, rabbit, dog and man. *Arzneimittelforschung*. 1985;35:1124–1132.
21. Ota H, Akishita M, Eto M, Iijima K, Kaneki M, Ouchi Y. Sirt1 modulates premature senescence-like phenotype in human endothelial cells. *J Mol Cell Cardiol*. 2007;43:571–579.
22. Albrecht EW, Stegeman CA, Heeringa P, Henning RH, van Goor H. Protective role of endothelial nitric oxide synthase. *J Pathol*. 2003;199:8–17.
23. Sato I, Morita I, Kaji K, Ikeda M, Nagao M, Murota S. Reduction of nitric oxide producing activity associated with in vitro aging in cultured human umbilical vein endothelial cell. *Biochem Biophys Res Commun*. 1993;195:1070–1076.
24. Takase H, Hashimoto A, Okutsu R, Hirose Y, Ito H, Imaizumi T, Miyakoda G, Mori T. Anti-atherosclerotic effect of cilostazol in apolipoprotein-E knockout mice. *Arzneimittelforschung*. 2007;57:185–191.
25. Nakamura T, Houchi H, Minami A, Sakamoto S, Tsuchiya K, Niwa Y, Minakuchi K, Nakaya Y. Endothelium-dependent relaxation by cilostazol, a phosphodiesteras III inhibitor, on rat thoracic aorta. *Life Sci*. 2001;69:1709–1715.
26. Watanabe K, Ikeda S, Komatsu J, Inaba S, Suzuki J, Sueda S, Funada J, Kitakaze M, Sekiya M. Effect of cilostazol on vasomotor reactivity in patients with vasospastic angina pectoris. *Am J Cardiol*. 2003;92:21–25.

Supplemental Figure Legends

Supplemental Figure I. BrdU incorporation and telomerase activity were restored by treatment with cilostazol (100 μmol/L) and DETA-NO (100 μmol/L). TSR-8, quantitation positive control template; H.S., heat shock sample for negative control. (unpaired t test, $^{*}p<0.05$ vs. cilo=0, N=3)

Supplemental Figure II. The effect of PKA and PI3K inhibitors on the cilostazol-induced phosphorylation of eNOS (Ser1177), Akt (Ser473) and expression of Sirt1. HUVEC were treated with cilostazol (100 μmol/L) with or without PKAI (1 μmol/L) or LY294002 (10 μmol/L) for 6hours.

Supplemental Figure III. A cell-free, horseradish peroxidase-coupled oxidation analysis about NAC or cilostazol. Data are shown as the mean ± S.E.M. of five experiments performed in duplicate. $^{*}p<0.05$.

Supplemental Figure IV. A. SA-βgal-positive cells were mostly located on the luminal surface. **B.** Urinary (Uri) 8-OhdG level (ng/mg creatinine) by treatment with cilostazol. **C.** Fluorescence micrographs with H_2O_2-sensitive DCF obtained from thoracic arteries treated with vehicle, paraquat or paraquat+cilostazol. $^{*}p<0.05$.

Supplemental Figure V. A. SA-ßgal staining of thoracic arteries from BALB/c mice administrated with cilostazol (60 mg/kg/day) at 7 days after treatment with STZ (60 mg/kg). **B.** Plasma glucose level at 3 days after the treatment. **C.** The number of SA-βgal-staining endothelial cells in cilostazol-treated thoracic arteries samples. (N=40, $^{*}p<0.05$).

Figure I

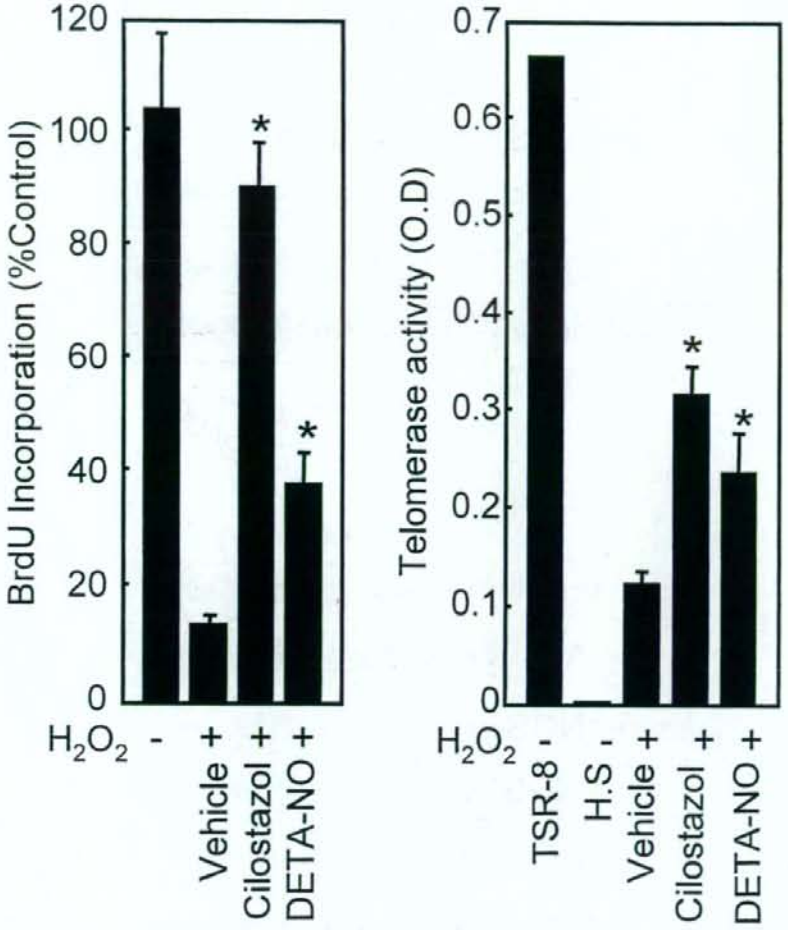
BrdU Incorporation (%Control)
120
100
80
60
40
20
0
*
*
H2O2 -
Vehicle +
Cilostazol +
DETA-NO +
Telomerase activity (O.D)
0.7
0.6
0.5
0.4
0.3
0.2
0.1
0
*
*
H2O2
TSR-8 -
H.S -
Vehicle +
Cilostazol +
DETA-NO +

Figure II

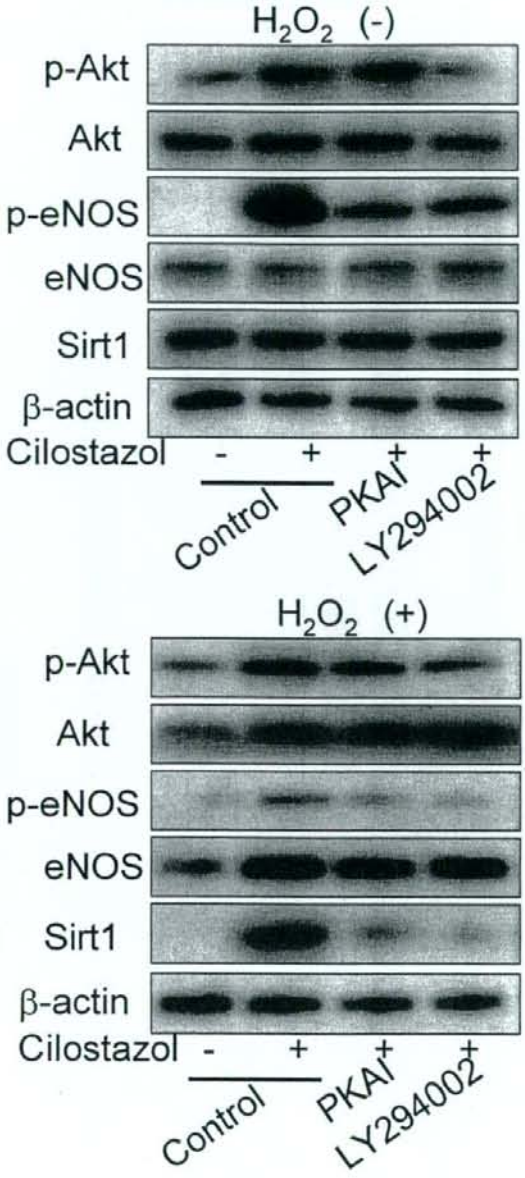
H2O2 (-)
p-Akt
Akt
p-eNOS
eNOS
Sirt1
β-actin
Cilostazol - + + +
Control
PKAI
LY294002
H2O2 (+)
p-Akt
Akt
p-eNOS
eNOS
Sirt1
β-actin
Cilostazol - + + +
Control
PKAI
LY294002

Figure III

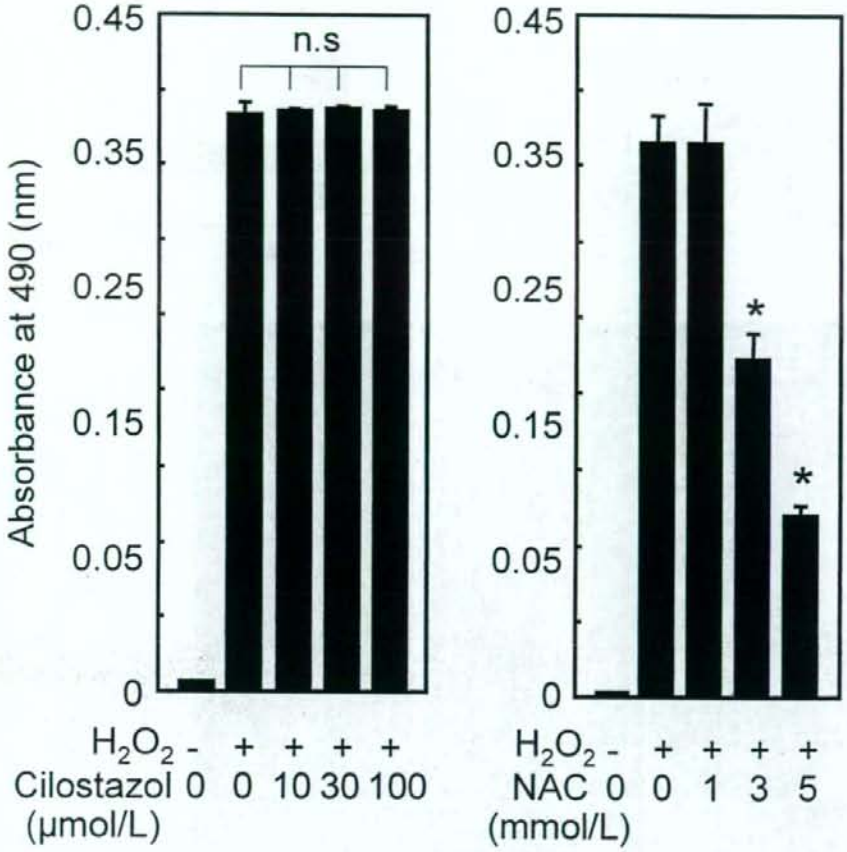
Absorbance at 490 (nm)
0.45
0.35
0.25
0.15
0.05
0
n.s
H_2O_2 - + + + +
Cilostazol 0 0 10 30 100
(μmol/L)
*
*
H_2O_2 - + + + +
NAC 0 0 1 3 5
(mmol/L)

Figure IV

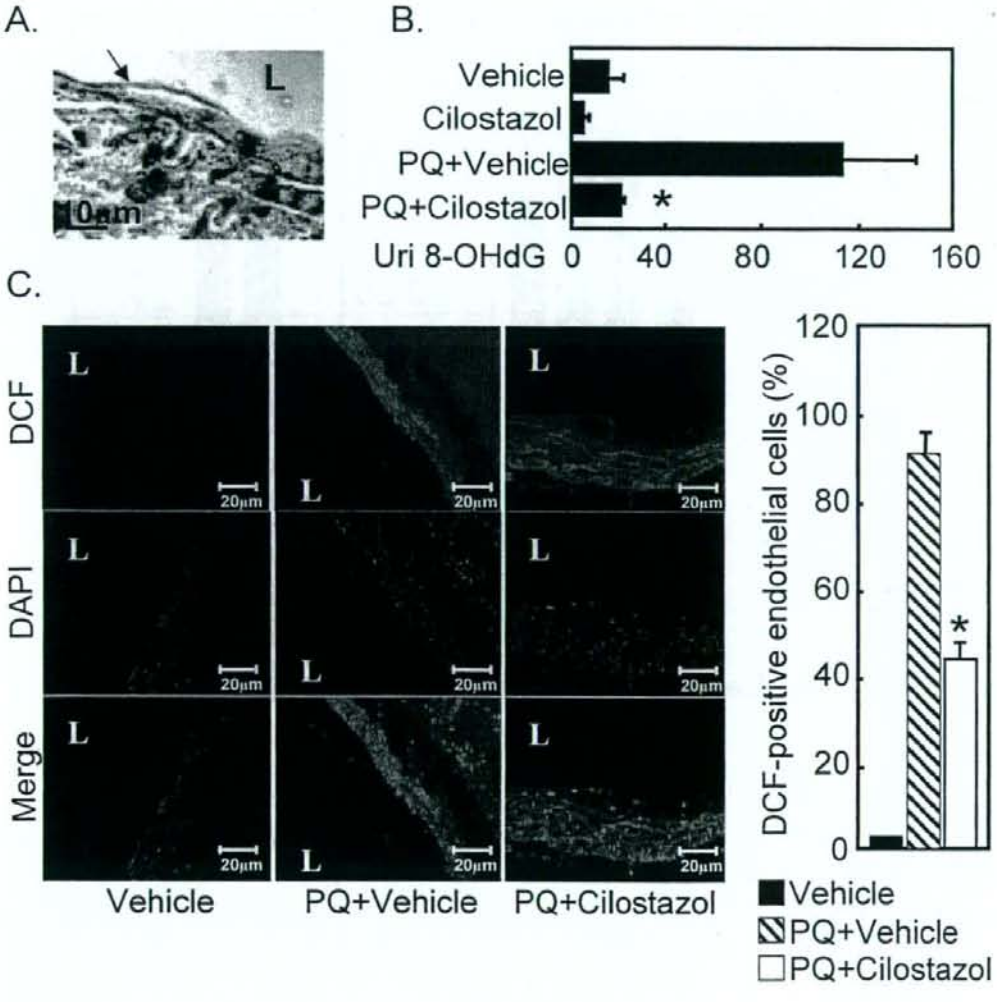
A.
L
0μm
B.
Vehicle
Cilostazol
PQ+Vehicle
PQ+Cilostazol
*
Uri 8-OHdG 0 40 80 120 160
C.
DCF
DAPI
Merge
L
20μm
Vehicle
PQ+Vehicle
PQ+Cilostazol
DCF-positive endothelial cells (%)
120
100
80
60
40
20
0
*
Vehicle
PQ+Vehicle
PQ+Cilostazol

Figure V

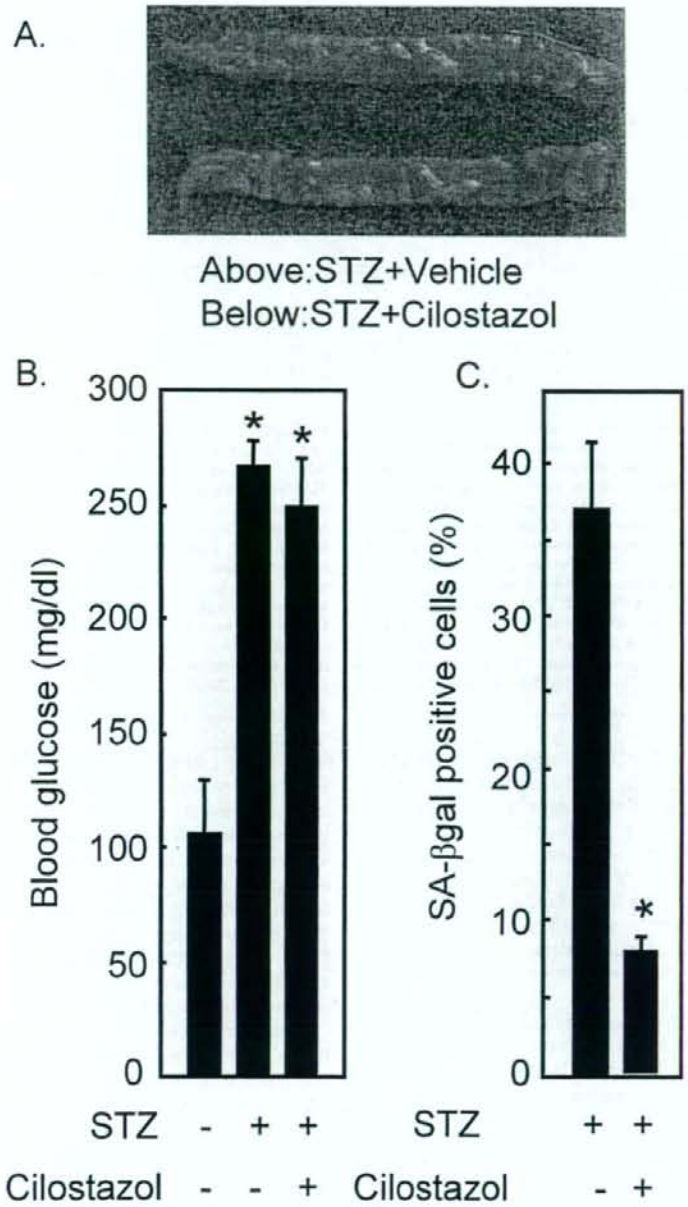
A.
Above:STZ+Vehicle
Below:STZ+Cilostazol
B.
Blood glucose (mg/dl)
300
250
200
150
100
50
0
*
*
STZ - + +
Cilostazol - - +
C.
SA-βgal positive cells (%)
40
30
20
10
0
*
STZ + +
Cilostazol - +

0013-7227/08/$15.00/0
Printed in U.S.A.

Endocrinology 149(4):1646–1653

doi: 10.1210/en.2007-1021

Adiponectin Antagonizes Stimulatory Effect of Tumor Necrosis Factor-α on Vascular Smooth Muscle Cell Calcification: Regulation of Growth Arrest-Specific Gene 6-Mediated Survival Pathway by Adenosine 5′-Monophosphate-Activated Protein Kinase

Bo-Kyung Son, Masahiro Akishita, Katsuya Iijima, Koichi Kozaki, Koji Maemura, Masato Eto, and Yasuyoshi Ouchi

Department of Geriatric Medicine (B.-K.S., M.A., K.I., M.E., Y.O.), the Department of Cardiovascular Medicine (K.M.), Graduate School of Medicine, The University of Tokyo, Tokyo 113-8655, Japan; and the Department of Geriatric Medicine (K.K.), School of Medicine, The University of Kyorin, Tokyo 181-8611, Japan

Adiponectin exhibits diverse protective effects against atherogenesis and antagonizes many effects of TNFα. Here, we investigated the effect of adiponectin and TNFα on vascular calcification, a critical event in the development and progression of vascular disease. In human aortic smooth muscle cells (HASMC), TNFα augmented inorganic phosphate (Pi)-induced calcification, whereas adiponectin significantly suppressed it and abolished the stimulatory effect of TNFα in a concentration-dependent manner. Similarly, adiponectin ameliorated the accelerating effect of TNFα on Pi-induced apoptosis, the essential process of HASMC calcification. Furthermore, these effects of TNFα and adiponectin were associated with AMP-activated protein kinase (AMPK)-dependent growth arrest-specific gene 6 (Gas6) expression and Akt signaling. The AMPK activator, 5-aminoimidazole-4-carboxamide ribonucleoside (AICAR), induced phosphorylation of AMPK and significantly inhibited Pi-induced calcification in HASMC. Conversely, pharmacological inhibition of AMPK by compound C blocked both AMPK activation and the inhibitory effect of adiponectin on calcification, providing evidence that AMPK plays a regulatory role in vascular calcification. Reporter assay revealed that adiponectin restored Gas6 promoter activity decreased by TNFα, and the effect of adiponectin was abrogated by compound C. These results demonstrate that adiponectin antagonizes the stimulatory effect of TNFα on vascular calcification by restoration of the AMPK-dependent Gas6-mediated survival pathway. (*Endocrinology* 149: 1646–1653, 2008)

VASCULAR CALCIFICATION is often encountered in advanced atherosclerotic lesions and is a common consequence of aging (1, 2). Calcification of the coronary arteries has been shown to be positively correlated with atherosclerotic plaque burden, increased risk of myocardial infarction, and plaque instability (3–5). We recently demonstrated that apoptosis plays an important role in inorganic phosphate (Pi)-induced vascular smooth muscle cell (VSMC) calcification (6). This type of calcification is dependent on down-regulation of the growth arrest-specific gene 6 (Gas6)-mediated survival pathway.

Adiponectin is an adipocyte-derived cytokine that exhibits protective properties in the heart and blood vessels (7–10). It accumulates in injured arteries from plasma and suppresses the endothelial inflammatory response (11) and VSMC proliferation (12). Furthermore, low plasma adiponectin levels are associated with progression of coronary artery calcification in type 1 diabetic and nondiabetic subjects, independent of other cardiovascular risk factors (13). Experimental studies have shown that adiponectin reduces TNFα production in response to various stresses, whereas TNFα attenuates adiponectin production, resulting in a reduction of plasma adiponectin levels (14–16). In addition to the inverse relationship between their expression, increasing evidence supports suppressive effects on each other's function (11, 17, 18). Given the importance of the reciprocal effects of TNFα and adiponectin, it is not clear whether both play a regulatory role in VSMC calcification.

Most of the beneficial actions of adiponectin are accounted for by the activation of AMP-activated protein kinase (AMPK) (19, 20). AMPK is a serine/threonine protein kinase that plays a key role in metabolic homeostasis in all eukaryotic cell types (21). Cardioprotective effects of adiponectin, including antiapoptotic actions, are also likely to be dependent on AMPK (19, 22, 23). However, the role of AMPK in the effect of adiponectin on VSMC calcification has not been addressed.

In the present study, we investigated whether adiponectin and TNFα modulate Pi-induced VSMC calcification by regulating apoptosis. We found that TNFα had a stimulatory effect, whereas adiponectin had an inhibitory effect on Pi-induced apoptosis and calcification in human aortic smooth muscle cells (HASMC). Furthermore, these actions were mediated by regulation of Gas6 at the transcription level via AMPK activation.

First Published Online January 3, 2008

Abbreviations: AICAR, 5-Aminoimidazole-4-carboxamide ribonucleoside; AMPK, AMP-activated protein kinase; Gas6, growth arrest-specific gene 6; HASMC, human aortic smooth muscle cells; Pi, inorganic phosphate; PP2C, protein phosphatase 2C; siRNA, small interfering RNA; TUNEL, terminal deoxynucleotidyl transferase-mediated dUTP nick end-labeling; VSMC, vascular smooth muscle cells.

***Endocrinology* is published monthly by The Endocrine Society (http://www.endo-society.org), the foremost professional society serving the endocrine community.**

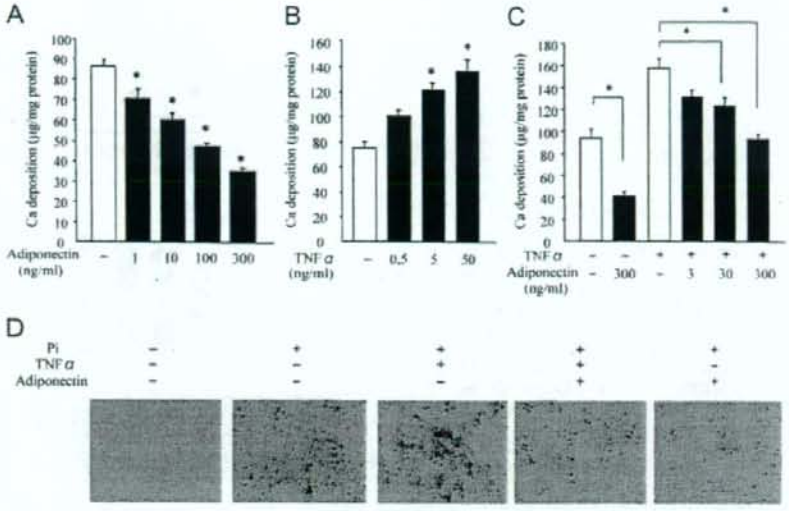

FIG. 1. Effect of adiponectin and TNFα on Pi-induced calcification. A and B, HASMC were cultured with the indicated concentrations of adiponectin (A) or TNFα (B) in calcification medium. They were added simultaneously when the medium was changed every 2 d. C, The effect of TNFα (20 ng/ml) and adiponectin with the indicated concentrations on Ca deposition was determined at 6 d. D, The effect of TNFα (20 ng/ml) and adiponectin (300 ng/ml) on Ca deposition was evaluated with von Kossa's staining at the light microscopic level. All values are presented as mean ± SE (n = 6). *, $P < 0.05$ by Bonferroni test. Each experiment was performed at least in triplicate for each condition.

Materials and Methods

Cell culture

HASMC were purchased from Clonetics Corp. (San Diego, CA). They were cultured in DMEM supplemented with 20% FBS, 100 U/ml penicillin, and 100 mg/ml streptomycin at 37 C in a humidified atmosphere with 5% CO_2. HASMC were used up to passage 8 for the experiments.

Induction and quantification of calcification

For Pi-induced calcification, Pi (a mixed solution of Na_2HPO_4 and NaH_2PO_4 whose pH was adjusted to 7.4) was added to serum-supplemented DMEM to a final concentration of 2.6 mM (calcification medium). Ca deposition was evaluated by the *o*-cresolphthalein complexone method (C-Test; WAKO, Osaka, Japan) and von Kossa's staining, as previously described (6, 24).

Determination of apoptosis

To examine the effect of TNFα (Sigma-Aldrich, St. Louis, MO) and adiponectin (R&D Systems, Minneapolis, MN) on Pi-induced apoptosis, they were added simultaneously when the medium was switched to the calcification medium. Apoptosis was detected by DNA fragmentation with a cell-death detection ELISA^{plus} kit (Roche, Manheim, Germany) and ter-

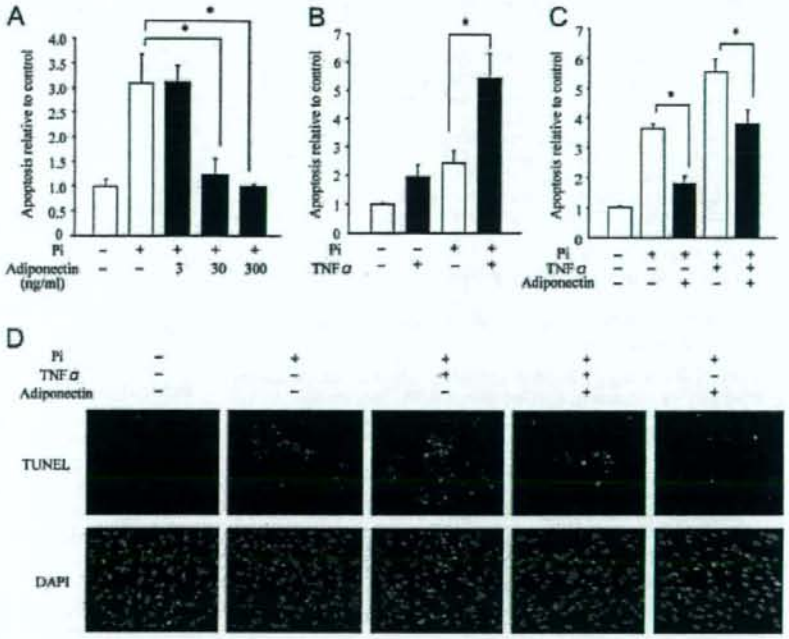

FIG. 2. Effect of adiponectin and TNFα on Pi-induced apoptosis. HASMC were cultured with the indicated concentrations of adiponectin for 6 d. Calcification medium was exchanged every 2 d. A, A quantitative index of apoptosis, determined by ELISA, is presented as the value relative to that without Pi treatment. B, HASMC were incubated with or without TNFα (20 ng/ml) in the absence or presence of 2.6 mM Pi for 6 d. C and D, On d 6, the effect of adiponectin (300 ng/ml) and TNFα (20 ng/ml) on apoptosis in calcification medium was determined by ELISA (C) and evaluated with TUNEL staining (D, *green*). Nuclei were counterstained with DAPI (*blue*). All values are presented as mean ± SE (n = 3). *, $P < 0.05$ by Bonferroni test. Each experiment was performed in triplicate for each condition.

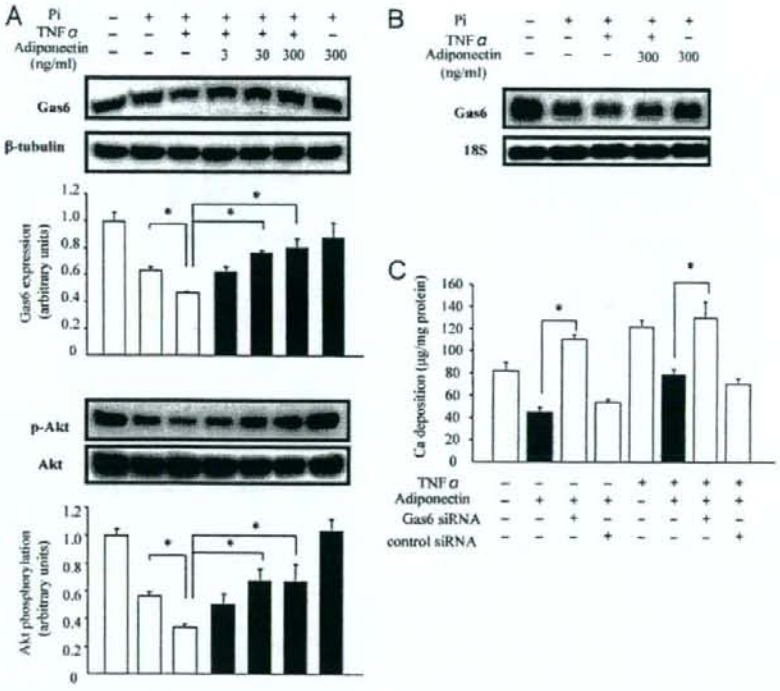

FIG. 3. Gas6 is the target of the effect of adiponectin and TNFα on Pi-induced calcification. HASMC were cultured with the indicated concentrations of adiponectin and TNFα (20 ng/ml). On d 6, cell lysates were collected and immunoblotted with antibodies that recognize Gas6, phospho-Akt (p-Akt), Akt, or β-tubulin. A, The untreated condition is the serum-supplemented status without Pi. B, Total RNA (5 μg) was harvested for Northern blot analysis after HASMC were incubated with adiponectin (300 ng/ml) and TNFα (20 ng/ml) for 6 d. When HASMC had reached 80–90% confluence, siRNA (100 nM) was transfected and then was transfected every 2 d with adiponectin (300 ng/ml) and TNFα (20 ng/ml) up to 6 d. C, Ca deposition was measured and normalized by cell protein content. All values are presented as mean ± SE (n = 3). *, $P < 0.05$ by Bonferroni test. Each experiment was performed in triplicate for each condition.

minal deoxynucleotidyl transferase-mediated dUTP nick end-labeling (TUNEL) assay with ApopTag Plus obtained from Chemicon International, Ltd. (Hampshire, UK), according to the manufacturer's instructions.

Generation of promoter reporter construct and luciferase activity assay

The 1925-bp Gas6 promoter (−1827/+99) corresponding to the Gas6 promoter sequences was generated by PCR from human genomic DNA with the appropriate sets of primers (6). These inserts were cloned into a pGL3 basic vector (Promega, Charbonnières, France) by standard molecular biological techniques. The construct was verified by sequencing. HASMC were transiently transfected in 12-well plates with 0.8 μg plasmid DNA and lipofectamine 2000 (Invitrogen Corp., Paisley, UK) according to the procedure recommended by the manufacturer. Cells were treated with TNFα, adiponectin, and compound C at 24 h after transfection, followed by incubation for an additional 44 h. Firefly luciferase activity was determined using a luciferase assay system (Promega) and normalized by total cell protein.

Preparation of small interfering RNA (siRNA) targeting Gas6 and transfection

To evaluate the role of Gas6 in the inhibitory effect of adiponectin on calcification, we knocked down Gas6 using siRNA. Two kinds of siRNA were designed to target human Gas6 and nonspecific control siRNA was synthesized using standard templates (6). siRNA (100 nM) was transfected using transfection reagent (Upstate, Charlottesville, VA) when HASMC had reached 80–90% confluence and then was transfected every 2 d with TNFα and adiponectin up to 6 d. The efficiency of Gas6 siRNA was confirmed with immunoblotting (6).

RNA extraction and Northern blot analysis

Total RNA was extracted from HASMC using an RNeasy minikit (QIAGEN, Courtaboeuf, France). For Northern blot analysis, harvested RNA (5 μg) was fractionated on 1.4% formaldehyde-agarose gel and transferred to a nylon filter. The filter was hybridized at 68 C for 2 h with ^{32}P-labeled Gas6 cDNA (6) and an 18S probe in QuickHyb solution (Stratagene, La Jolla, CA) and autoradiographed.

Immunoblotting

The effect of TNFα and adiponectin on the expression of Gas6, phospho-Akt, and Akt was examined, as described previously (24). Analysis of AMPK activation was performed using an antibody specific for the phosphorylated Thr172 of AMPK (Cell Signaling Technology Inc., Beverly, MA).

Statistical analysis

All results are presented as mean ± SE. Statistical comparisons were made by ANOVA, followed by Bonferroni test. A value of $P < 0.05$ was considered statistically significant.

Results

Adiponectin and TNFα regulate Pi-induced calcification in HASMC

To investigate the effect of adiponectin and TNFα on Pi-induced calcification, HASMC were incubated with adiponectin and TNFα in the presence of 2.6 mM Pi. On d 6, Ca deposition was suppressed by adiponectin in a concentration-dependent manner (40 ± 2% of control at 300 ng/ml, Fig. 1A), whereas TNFα significantly augmented Ca deposition (182 ± 13% of control at 50 ng/ml; Fig. 1B). Furthermore, adiponectin clearly inhibited Ca deposition stimulated by TNFα in a concentration-dependent manner (Fig. 1C). This was also found by von Kossa's staining (Fig. 1D). These results suggest that adiponectin has an inhibitory effect on both Pi-induced and TNFα-stimulated calcification in HASMC.

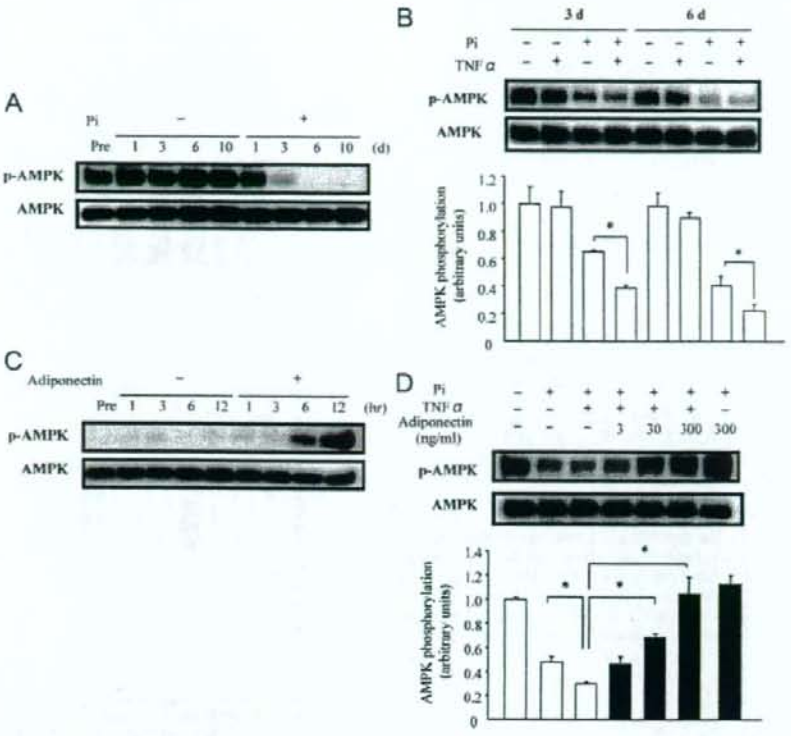

FIG. 4. Effect of adiponectin and TNFα on AMPK activity during Pi-induced calcification. HASMC were cultured in the absence or presence of Pi (2.6 mM) for up to 10 d. After the indicated incubation period, cell lysates were harvested and immunoblotted with antibodies to phospho-AMPK (p-AMPK) and AMPK. A, The untreated condition is the serum-supplemented status without Pi. B, Immunoblotting analysis showing the effect of TNFα (20 ng/ml) on p-AMPK and AMPK expression in the absence or presence of serum containing Pi (2.6 mM). C, Serum-starved HASMC were incubated with or without adiponectin (300 ng/ml) for 12 h. HASMC were cultured with the indicated concentrations of adiponectin and TNFα (20 ng/ml). D, On d 6, cell lysates were harvested and immunoblotted with antibodies to p-AMPK and AMPK. All values are presented as mean ± SE (n = 3). *, $P < 0.05$ by Bonferroni test. Each experiment was performed in triplicate for each condition.

Adiponectin antagonizes stimulatory effect of TNFα on Pi-induced apoptosis by restoration of Gas6-mediated survival pathway

Because apoptosis has been shown to be an important pathway regulating Pi-induced calcification (6, 24), we examined the effect of adiponectin and TNFα on apoptosis in HASMC. Adiponectin, at concentrations exerting inhibitory effects on calcification, significantly reduced apoptosis, as quantified by cytoplasmic histone-associated DNA fragments (Fig. 2A). On the other hand, apoptosis was enhanced by TNFα in the presence of Pi (Fig. 2B). As shown in Ca deposition, adiponectin antagonized the stimulatory effect of TNFα on apoptosis. This inhibition was also observed by TUNEL assay (Fig. 2, C and D).

We previously demonstrated that Pi-induced apoptosis was mediated by down-regulation of the Gas6-mediated survival pathway (6, 24). Therefore, we examined the effects of adiponectin and TNFα on this pathway. Both Gas6 mRNA and protein expression were down-regulated by TNFα in the presence of Pi, whereas adiponectin clearly restored their expression (Fig. 3, A and B). Next, because the Gas6-mediated survival pathway is Akt-dependent, the effect of adiponectin and TNFα on Akt phosphorylation was examined. As shown in the Gas6 expression, the similar effect of adiponectin and TNFα was observed in Akt phosphorylation that is high at basal level in the untreated condition containing serum (Fig. 3A). We confirmed that total Akt was not changed by adiponectin and TNFα treatment (Fig. 3A). On the other hand, adiponectin and TNFα did not affect Gas6 expression and Akt phosphorylation in the condition without Pi treatment (data not shown).

Furthermore, to evaluate the role of Gas6 in the inhibitory effect of adiponectin on calcification, we examined whether the knockdown of Gas6 abrogated the effects of adiponectin using siRNA. On d 6, transfection of Gas6 siRNA markedly decreased its expression (data not shown), as reported previously (6). The inhibitory effect of adiponectin on Pi- and TNFα-induced calcification was reversed by Gas6 siRNA, supporting the critical role of Gas6 in the effect of adiponectin on calcification (Fig. 3C).

AMPK plays a critical role in VSMC calcification and is regulated by adiponectin and TNFα

It has been reported that AMPK is a central signaling molecule in adiponectin's action (19, 20). We investigated whether AMPK is involved in the effect of adiponectin on Pi-induced calcification. First, we examined the activity of AMPK during calcification. Immunoblot analysis showed that phosphorylated AMPK was markedly down-regulated in the presence of Pi for 10 d, whereas the expression of total AMPK was not changed (Fig. 4A). TNFα further inhibited its phosphorylation in the presence of Pi, without changing total AMPK (Fig. 4B). In the case of adiponectin, AMPK phosphorylation was remarkably stimulated in a time-dependent manner (Fig. 4C). As shown in Fig. 4D, adiponectin further restored AMPK phos-